SMiRT-12 / K. Kussmaul (Editor)



E10/3

# FLUID ELASTIC INSTABILITY ANALYSIS OF 1/6TH EXPERIMENTAL MODEL OF PFBR MAIN VESSEL COOLING CIRCUIT

S. Jalaldeen, R. Ravi, P. Chellapandi and S.B. Bhoje

Nuclear Systems Division, Indira Gandhi Centre for Atomic Research, Kalpakkam, India

## 1 INTRODUCTION

In reactor assembly of Prototype Fast Breeder Reactor (PFBR) (Fig.1), the main vessel (MV) temperature is kept below creep range ie. less than 427 deg C by way of diverting a small fraction of core flow from the cold pool and sent through the passage between main vessel and an outer cylindrical baffle to cool the vessel. The sodium coming from this, is collected by another inner baffle and then returned to cold pool again. This system is termed as MV cooling circuit (Fig.2). The outer and inner baffles form feeding and restitution collectors respectively. The sodium from the feeding collector flows over the outer baffle and falls through a height of about 0.5 m before impacting on the free surface of sodium in the restitution collector. The fall of sodium may become a source of vibration of the baffles. Such vibrations have been already noted in case of SPX-1 during its commissioning stage [Aita.S. 1986].

For PFBR, the theoretical analysis was done to assess the fluid-elastic instability risks and stability charts were obtained. By this, it was concluded that the operating point (flow rate and fall height) lies within the stable zone (Jalaldeen.S 1991). In order to confirm the above analysis results, a series of experiments were proposed. One preliminary experiment on 1/16 th model of MV cooling circuit has been completed [Premnath.J. 1991]. This model has also been analysed theoretically for the fluid-elastic instability. The theoretical analysis involves 2 stage computations. In the first stage, free vibration analysis with fluid structure interaction (FSI) effect for experimental model has been done using INCA (CASTEM 1985) code and all the mode shapes including sloshing are extracted. In the second stage the instability analysis is performed with the free vibration results from INCA. For the instability computations, a code WEIR has been written based on Aita's instability criteria [Aita.S. 1986].

## 2 THEORETICAL BACK GROUND

### 2.1 Types of weir instability mechanisms

There are two types of mechanisms involved in the instability of the weir system, viz. type-1 and type-2 mechanisms. The type-1 mechanism concerns with sloshing modes of the free surfaces of the feeding and restitution

collectors and is due to strong coupling between two thin collectors (feeding and restitution) because of very flexible shell in between them. Type-2 mechanism is mainly due to the fluid structure interaction. This occurs at high flow rate and high fall heights. The frequency corresponding to this mechanism is much higher than that of type-1 mechanism. The mathematical description given by (Aita.S 1986) was suitably adopted for PFBR application (Jalaldeen.S 1991).

### 2.2 Stability Analysis methodology

The methodology adopted for solving the instability problem involves following 3 steps:

step 1 : Free vibration analysis including fluid-structure interaction effect for each circumferential wave number 'n'. This has been done with 'INCA'.
step 2 : Computation of non-dimensional delay time and impact velocity.
step 3 : Applying the Aita's instability criteria.

Steps 1 - 3 are repeated for each wave number 'n'

The above steps are automatically executed by the post processor routine called 'WEIR' using the results from 'INCA'. This program also gives graphical output of sloshing mode shapes.

## 3 EXPERIMENTAL STUDY OF 1/16 TH MODEL

### 3.1 Model Details

The 1/16th model of main vessel weir cooling system (Fig.3) consists of one thick (10 mm thick) shell inside which there are two thin shells of each 0.5 mm thick. The inner two thin shell are called outer and inner baffles. Outer baffle is bolted to the 10 mm thick shell and the inner baffle is welded to the outer baffle as shown in figure. The two baffles form feeding and restitution collectors. The feeding collector has 30 holes at its bottom for water inlet and similar and same number of holes are provided at the bottom of the restitution collector for water outlet. The inlet valve controls the flow rate whereas the outlet valve controls the fall height. The water coming from the restitution collector joins a large pool of water inside the inner baffle. This central pool of water has an outlet pipe. The flow rate is varied from 0.0 to 3.5 cu.m/hr in steps of 0.5 cu.m/hr. For each flow rate, the fall height is varied from 0.0 to 130 mm in steps of 10 mm. More details of the experiments and the results are given in the companion paper (Premnath.J. 1993)

### 3.2 Results of experimental analysis

The experimentally obtained instability chart drawn using experimental data is shown in Fig.4. The circumferential wave number for the most critical zone is found to be 9 with the associated frequency of 6 Hz and hence the instability appears to be FSI type, i.e. type-2 mechanism. In the very low flow rate (0.25 cu m/hr) and fall height (almost 0.001 m), there appears to be a sloshing type of instability.

In general, the parameters, like surface roughness, damping factor and weir shell constant which are required for the theoretical analysis have to be determined experimentally. Out of this the weir flow constant has been assumed as 0.5 from the open literature. The surface roughness measured is 0.15 - 0.7 microns and damping factor measured is 3.0 - 6.0 %. For the analysis average values have been used.

## 4 THEORETICAL ANALYSIS

### 4.1 Free Vibration Analysis

Free vibration analysis is done for the 1/16 th model of weir system using 'INCA'. The FEM model is shown in Fig.6. Sodium is modelled using 452 four noded liquid elements. Structure is modelled using 87 two noded axisymmetric shell elements. The connection between the shell and the liquid is modelled by 115 fluid-structure interaction elements. The free surfaces are modelled by 16 surface elements. The bottom of both the baffles are assumed to be connected rigidly to the outer shell. The results of free vibration analysis is given in Table 1. The sloshing mode shape is shown in Fig.7.

Table 1 Extracts from free vibration analysis of 1/16 th model

| Circumferential wave number(n) | $\omega_1$ Hz | $\omega_2$ Hz | $\Delta f$ Hz | $\Delta\Omega^{**}$ Hz | $\omega_{nm}$ Hz | $Znm^{(1)}/Znm^{(2)}$ |
|---|---|---|---|---|---|---|
| 1 | 0.544 | 0.647 | 0.103 | 0.170 | 12.890 | -16.00 |
| 2 | 0.969 | 1.050 | 0.081 | 0.080 | 12.890 | -9.00 |
| 3 | 1.267 | 1.298 | 0.031 | 0.024 | 10.130 | -9.00 |
| 4 | 1.482 | 1.496 | 0.014 | 0.009 | 7.756 | -6.00 |
| 5 | 1.640 | 1.674 | 0.034 | 0.021 | 6.695 | -1.33 |
| 6 | 1.769 | 1.845 | 0.076 | 0.042 | 6.026 | -0.50 |
| 7 | 1.891 | 2.006 | 0.115 | 0.059 | 5.630 | -0.33 |
| 8 | 2.027 | 2.157 | 0.130 | 0.062 | 6.667 | -0.30 |
| 9 | 2.181 | 2.298 | 0.117 | 0.052 | 6.088 | -0.30 |
| 10 | 2.339 | 2.436 | 0.097 | 0.041 | 6.785 | -1.00 |

** $\Delta\Omega = \left(\frac{2 \cdot \Delta f}{\omega_1 + \omega_2}\right)$

### 4.3 Stability Analysis

The delay time and impact velocity of the film are computed taking the roughness of the wall surface into account. The velocity profile along the fall height for a typical flow rate of 0.25 cu.m3/hr with surface roughness of 0.35 microns and weir constant of 0.5 is shown in Fig.5. The average overflow velocity is assumed as the downward velocity at the weir crest (V1).

The program 'WEIR' was used to get the stability chart in flow rate and fall height domain for each significant circumferential wave numbers 'n'.

### 4.4 Analysis Results

The theoretically obtained stability chart is shown in Fig.8. There is

overlapping of type-1 & 2 mechanisms which is shown in Fig.8. The circumferential wave number corresponding to the critical instability zone is 9, whose associated frequency is 6 Hz. The type-2 mechanism is found to be very critical and further type-1 mechanism is possible for higher flow rates & fall heights. The charts for other wave numbers are also included in the Fig.7. From Fig.7, the most critical instability zone is extracted and the same has been compared with the experimental predictions in Fig.8. The experimentally determined instability points are all lying well within the theoretically predicted zone of instability. This demonstrates that the theoretical predictions are conservative.

## 5 CONCLUSION

The instability of weir system is studied theoretically as well as experimentally for 1/16th model of MV cooling circuit and the results are compared. The theoretical prediction of instabilty zones is conservative, i.e. all the experimental data points are lying well with in the theoretically predicted instability region. This zone corresponds to the circumferential wave number of 7 - 9.

The discrepancies between experimental and theoretical are due to the following reasons:

a. Lack of axisymmetric flow over the weir shell crest.
b. Lack of uniformity in the gap between baffles.
c. Effect of hot pool on the instability.
d. Improper wedge profile. This does not permit the falling fluid to have perfect wetting on the weir shell. Theoretical prediction is based on perfect wetting.

## 6 REFERENCES

Aita.S., Gibert.R.J, Verrier.P, Bertaut.C, Lacroix.C, D'onghia.E. (1986). Vibratory instability in Super Phenix LMFBR discovery and solution. IWGFR Specialist meeting on FIV in FBRs. No IWGFR 62

Aita.S, Gibert R.J. (1986). Fluid-elastic instability in a flexible weir. Flow induced vibration PVP-Vol.104.

CASTEM-INCA (1985). A 2-D finite element code for structural analysis. CEN/DMT, Saclay, France.

Jalaldeen.S. Balasubramaniyam.V, Chellapandi.P, Bhoje.S.B, (1991). Fluidelastic instability analysis for PFBR mainvessel cooling circuit. SMiRT-11,vol.E

Jason Premnath, Prabhakar.R, Kale.R.D. (1991). Experimental analysis of 1/16 th model of weir cooling system of PFBR. IGCAR Internal note.

Jason Premnath, Thirumalai.M, Prabhakar.R, Kale.R.D. (1991). Experimental study of flow induced vibration of thermal baffles of PFBR. SMiRT-12, vol.E, Paper E10/4.

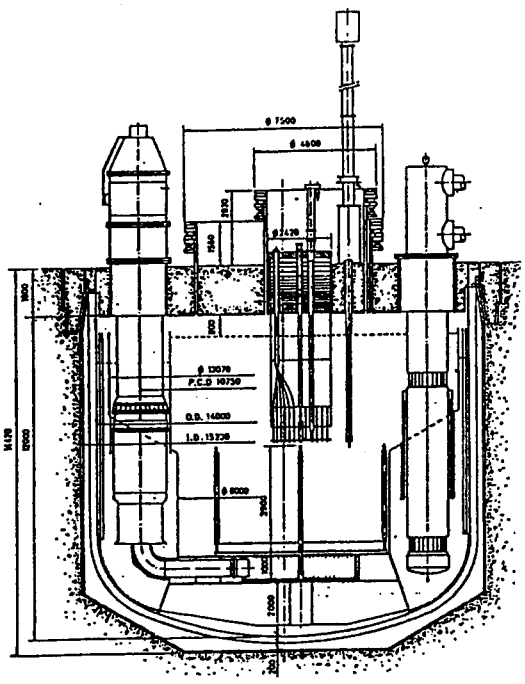

Fig1. PFBR Reactor assembly

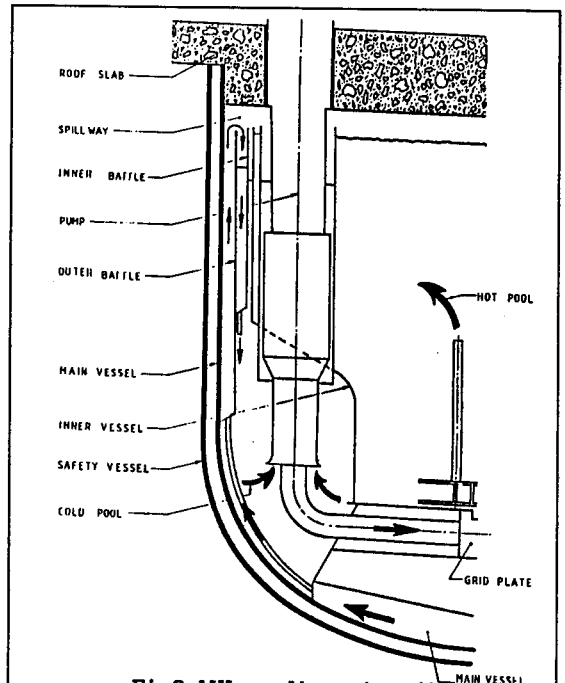


Fig2. MV cooling circuit

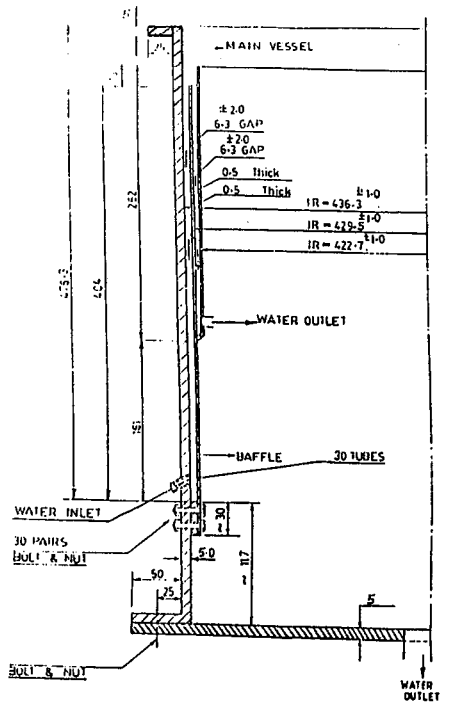


Fig3. Experimental model

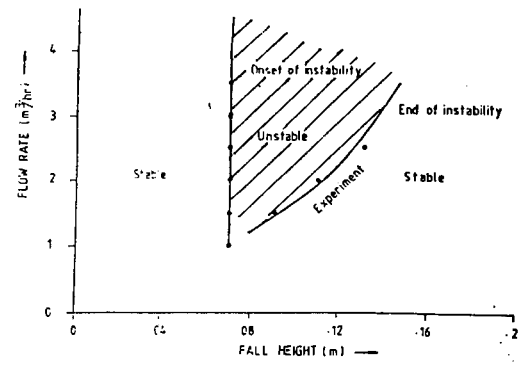


Fig4. Experimental results

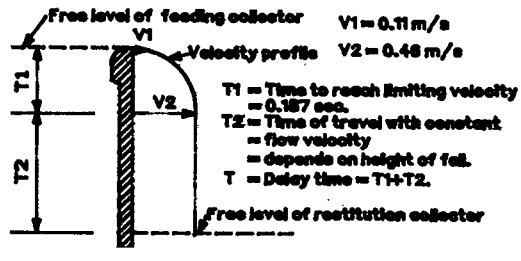


Fig5. Velocity profile

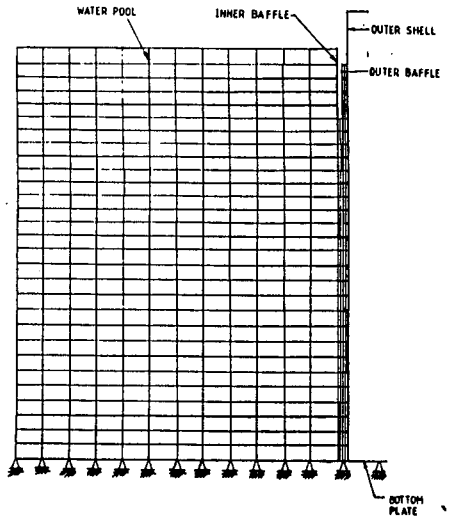


Fig6. FEM mesh

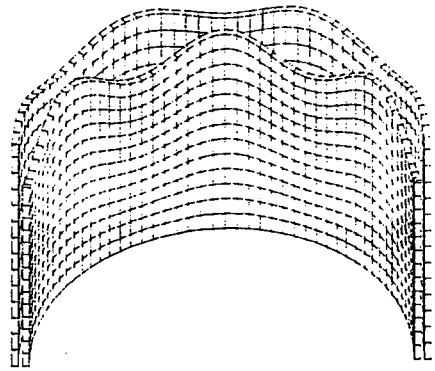

Fig7. Sloshing mode from weir

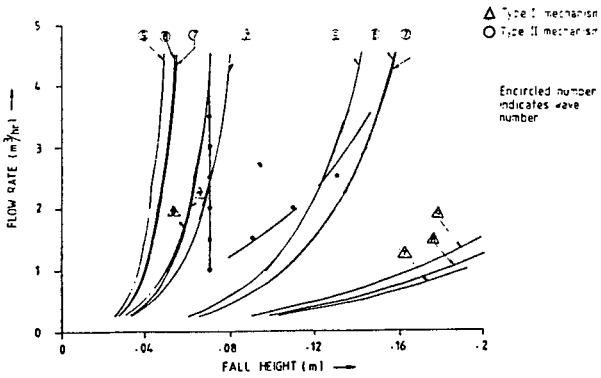


Fig8. Results of instability analysis

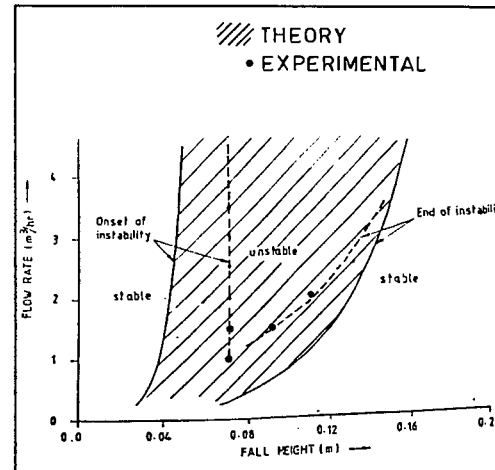


Fig9. Comparision of experimental and theoritical results